

Polysoaps: Extension and Compression

O. V. Borisov

Max Planck Institut für Polymerforschung, 55021 Mainz, Germany

A. Halperin*

ICSI, 15 rue Jean Starcky, BP 2488, 68057 Mulhouse, France

Received November 12, 1996; Revised Manuscript Received April 14, 1997[®]

ABSTRACT: Intramolecular self-assembly in polysoaps qualitatively modifies their deformation behavior. The modified elasticity reflects the coupling of the chain deformation to the internal degrees of freedom associated with the existence of intrachain micelles. The equilibration of this secondary structure tends to lower the restoring force associated with the deformation in accordance with the LeChatelier principle. The force laws for extension and for confinement into a slit are derived for the case of a linear string of spherical intrachain micelles. In both situations the chain behaves as a string of stars for weak deformations. Force laws characteristic of simple linear chains are obtained for strong deformations. Novel force laws, reflecting strong coupling to the secondary structure, are obtained at the intermediate regime. For intermediate extensions, the tension in the chain, f , is independent of R , the end to end distance, up to logarithmic corrections, *i.e.*, $f \sim R^0 \ln g(R)$, where $g(R)$ is a slowly increasing function of R . For intermediate confinement $f \sim D^{-28/23}$, where D is the spacing between the two nonadsorbing walls.

I. Introduction

The elasticity of flexible polymers is, possibly, their most notable attribute. It plays a key role in a variety of important phenomena such as rubber elasticity,^{1,2} colloidal stabilization by adsorbed chains,³ rheology,⁴ *etc.* The essential physics of this entropic elasticity were formulated between 1936 and 1943 by Kuhn,⁵ Kuhn and Gr \ddot{u} n,⁶ Guth and Mark,⁷ and by James and Guth.⁸ Qualitative modifications of this picture are necessary when the flexible chain incorporates numerous associating groups, "stickers".^{9,10} The modifications are required because of intrachain associations that give rise to a "secondary structure". In turn, this strongly affects the configurations and the elasticity of the flexible coils. The deformation of such polymers induces rearrangement of the secondary structure, thus leading to novel force laws. In the following we present a simple theory describing the extension and the confinement behavior of a particular family of associating polymers: polysoaps.¹¹ These are flexible polymers whose hydrophilic backbone incorporates, at intervals, m covalently bound, amphiphilic monomers. In water, the polymerized amphiphiles self-assemble into intrachain micelles. In the following we limit the discussion to the case of *spherical* intrachain micelles with an aggregation number p_{eq} . This level of self-organization corresponds to a secondary structure. The discussion is further limited to long polysoaps, $m/p_{eq} \gg 1$, that self assemble into a *linear* string of intrachain micelles (Figure 1). Our concern is with the force laws characterizing the deformation behavior of polysoaps when the hydrophilic backbone experiences an athermal good solvent. In particular, we consider the *extension* of isolated polysoaps and their *confinement* into slits (Figure 2). In both cases we may distinguish between three rough regimes. For weak deformations, the polysoaps behave, essentially, as a string of stars. The micellar structure is hardly perturbed. Strong deformations are characterized by force laws typical of the fully dissociated, linear chains. However, at intermediate deformations, the secondary structure is affected, thus giving rise to novel force laws. As we shall see, the stretching

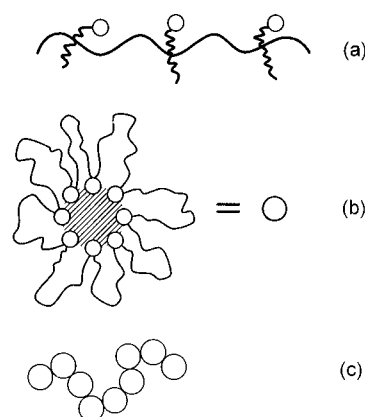


Figure 1. Polysoaps comprising amphiphilic monomers joined by flexible, hydrophilic spacer chains, exhibiting a hierarchy of intrachain self-organization. The monomer sequence (a), the "primary structure", is imposed by the synthesis. The polymerized amphiphiles self-assemble into intrachain micelles (b), thus giving rise to a secondary structure. In long polysoaps, a tertiary level of self-organization is associated with the configurations of the string of micelles. In this article, we only consider the case of a linear string of spherical intrachain micelles.

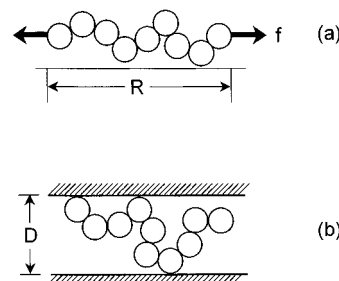


Figure 2. Deformation of a linear string of micelles for two situations: (a) extension and (b) confinement between two nonadsorbing walls.

behavior is especially striking.^{9,10} At intermediate extensions the strain is independent of the stress up to logarithmic corrections. Apart from the fundamental interest in the elasticity of polymers possessing secondary structure, the problem is also of practical importance. This is due to the wide spread utilization of

[®] Abstract published in *Advance ACS Abstracts*, June 15, 1997.

polysoaps as viscosity modifiers and colloidal stabilizers. Understanding their extension behavior should prove useful in the interpretation of the rheology of polysoap solutions. The confinement behavior is relevant to the understanding of their adsorption behavior.

The incorporation of amphiphilic monomers into the flexible, hydrophilic chain gives rise to qualitatively distinctive configurations.^{12,13} What was a featureless random coil exhibits a hierarchy of self-organization. The monomer sequence may be regarded as a primary structure. As noted above, the intrachain micelles may be considered as a secondary structure. When $m \approx p_{eq}$, there is no higher level of self-organization. However, for long polysoaps we may also distinguish a "tertiary" structure. In this case the individual chain self-assembles into numerous, $m/p_{eq} \gg 1$, intrachain micelles. The tertiary structure corresponds to the various possible configurations of the string of micelles. Three extreme situations may be envisioned: a linear string, a branched one,¹² and a collapsed, globular state.¹³ Of these, the collapsed configuration corresponds to the stable equilibrium. However, other configurations are expected to occur as long-lived, metastable states. We limit the discussion to the simplest case, of a linear string comprising spherical intrachain micelles. This configuration does not correspond to a stable equilibrium. However, some of the regimes obtained in the analysis of the linear string are expected to occur irrespective of the initial configuration of the polysoap. In addition, it is of interest to understand the linear string case because it may occur experimentally as a metastable state. Altogether, our discussion concerns long polysoaps incorporating $m \gg 1$ amphiphiles. It is limited to the case of amphiphiles joined by long, flexible *spacer chains*. Each spacer consists of n monomers such that $N \gg n \gg 1$ where $N \approx nm$ is the overall polymerization degree of the chain. It is assumed that all the amphiphiles are self-assembled into micelles when the chain is unperturbed. We focus on the behavior of polysoaps in an aqueous medium of high ionic strength so as to screen long-range electrostatic interactions. Water is considered as an athermal good solvent for the hydrophilic backbone. The discussion utilizes a scaling approach and numerical prefactors are thus ignored.

Before we proceed, it is helpful to begin with some remarks about associating polymers in general. Their phenomenology is largely determined by three parameters: The number of associating moieties, their functionality, and the strength of the association. Of these parameters, the number of stickers, m , dominates the single chain behavior. No effect is expected when $m = 1$. For $m = 2$ the single chain behavior is weakly modified by the formation of a loop or a ring. A fully developed secondary/tertiary structure is expected for $m \gg 2$. In the above terms, polysoaps are associating polymers incorporating numerous, multifunctional, weak stickers. The functionality of the amphiphilic stickers is, essentially, the aggregation number of the intrachain micelles, p_{eq} . The comparative weakness of the associations ensures that the intrachain micelles attain equilibrium. It also enables the much slower equilibration of the overall chain configuration. This brings us to some general observations regarding the thermodynamics of the elasticity of associating polymers incorporating $m \gg 2$ stickers. For simple flexible polymers the tension in the extended chain, f , is characterized by two traits. First, f is a function of two independent variables, the end to end distance, R , and the temperature, T , $f =$

$f(R, T)$. This is reminiscent of the equation of state of a gas, $P = P(V, T)$. Second, familiar polymers tend to stiffen when subjected to strong deformation. The "spring constant" characterizing their elastic response may only increase with R ; i.e., $d f/d R$ can increase with R but does not decrease. Both characteristics are modified in the case of associating polymers. In such a case the force law is of the form $f = f(R, T, \psi(R, T), p(R, T))$, where ψ is the fraction of associated stickers and p is their average aggregation number. The deformation behavior of the associating polymers reflects the LeChatelier principle:¹⁴ External interactions that disturb the equilibrium of the system bring about processes that tend to reduce the effect of the interactions. In particular, the internal degrees of freedom, ψ and p , equilibrate so as to lower f , i.e., $(\partial f / \partial R)_{\psi, p = \text{const}'} > (\partial f / \partial R)_{eq}$. One may gain insight regarding the situation by comparing the extension of the polymers to the compression of a gas. The extension of a flexible homopolymer is reminiscent of the isothermal compression of a single-component gas. The number of Kuhn lengths in the chain is independent of R . Similarly, the number of gas molecules is independent of the volume, V . The extension of an associating polymer is comparable to the isothermal compression of a reactive mixture of gases in equilibrium, for example $O_2 + 2H_2 \rightleftharpoons 2H_2O$.¹⁵ As the gas is compressed, the equilibrium is shifted toward the right and the number of gas molecules in the system decreases. As a result, the pressure of the compressed mixture is lower in comparison to the case of a single-component gas. Similar effects occur in stretched associating polymers due to the relaxation of the secondary structure, $\psi(R, T)$ and $p(R, T)$. The number of effective Kuhn lengths in the chain increases so as to lower f in comparison to f of "simple" flexible chains.

These general observations capture the distinctive features of the thermodynamics of the elasticity of polysoaps. However, in order to obtain a particular force law it is necessary to consider the statistical mechanics of a specific system. The model adopted for unperturbed polysoaps is described in section II. Section III is devoted to the extension behavior of polysoaps, allowing only for uniform reduction in the aggregation number of the micelles. The resulting fR diagram exhibits a van der Waals loop, suggesting a coexistence of weakly perturbed micelles and fully dissociated amphiphiles. The fR diagram allowing for this coexistence is derived and discussed in sections IV and V. Initially, in section IV, we ignore the role of S_{mix} , the mixing entropy of the one-dimensional solution of micelles and the dissociated amphiphiles. Within this approximation the behavior at coexistence is reminiscent of a first-order phase transition and $f \sim R^0$. Two approaches are used. One utilizes a $T = \text{const}'$, $R = \text{const}'$ ensemble. It adapts our earlier analysis^{9,10} to the case of a backbone immersed in a good solvent. The second approach involves the use of a $T = \text{const}'$, $f = \text{const}'$ ensemble. It justifies some of the approximations used in the first derivation and casts the results in a somewhat different form. The role of S_{mix} is explored in section V. It is found to "smear" the features reminiscent of a first-order phase transition. The plateau $f \sim R^0$ is replaced by logarithmic R dependence $f \sim \ln g(R)$, where $g(R)$ is a weakly increasing function of R . The crossovers to the fully micellized and fully dissociated regimes become smooth. S_{mix} also sets a bound on the m values for which we may assume that the unperturbed chain is fully micellized. Section VI

is devoted to the confinement of polysoaps to a slit of width D formed by nonadsorbing, flat walls. In this case, the picture of a uniform string of micelles is applicable and no coexistence is involved. However, a novel, $f \sim D^{-28/23}$, force law is found for intermediate confinements. Also, the aggregation number is found to vary nonmonotonously as the compression increases.

II. Unperturbed Polysoap

The self-assembly of the polymerized amphiphiles results in a major modification of the configurations of the chain.^{12,13,16} The initially featureless coil develops a hierarchy of intramolecular self-organization. Intrachain micelles are the elementary units of the self-assembled polysoap. Structurally, these micelles are similar to micelles formed by free, unpolymerized amphiphiles. The hydrophobic tails of the amphiphiles form a dense, meltlike, core with the head groups straddling the boundary. An additional feature, distinctive to this system, occurs because the amphiphiles are joined by long, flexible spacer chains. Upon aggregation, these fold back, thus giving rise to a swollen corona of loops surrounding the "bare micelle" (Figure 1). Our description of the intrachain micelles is based on the combination of two models: the model of Israelachvili *et al.* for micelles of free amphiphiles¹⁷ and the Daoud–Cotton¹⁸ model for star polymers. The former describes the inner region of aggregated amphiphiles. The latter depicts the surrounding, starlike corona. The main features of the Daoud–Cotton model, for free as well as for confined stars, are described in Appendix I. The essentials of the model of Israelachvili *et al.* are as follows. The free energy per amphiphile consists of three terms: (i) The transfer free energy, $-\delta kT$, of the hydrophobic tail from water into the micellar core. (ii) The surface free energy due to the contact between the hydrophobic core and the surrounding water. This term is of the form γkTa , where a is the surface area per head group and γkT is the surface tension of the core–water interface. It favors micellar growth. (iii) A penalty term due to the repulsive interactions between the head groups. Since the number of binary "contacts" between one head group and its neighbors is proportional to the surface density, $1/a$, this term scales as $1/a$. It opposes micellar growth. The free energy per surfactant in a free micelle of aggregation number p , $\tilde{\epsilon}_p kT$, is thus

$$\tilde{\epsilon}_p \approx \gamma a_0(a/a_0 + a_0/a) - \delta \quad (1)$$

where a_0 is the optimal, equilibrium area per head group. For spherical micelles p is related to the volume of the hydrophobic tail, v , as $p \approx v^2/a^3$ and the equilibrium aggregation number is thus

$$p_0 \approx v^2/a_0^3 \quad (2)$$

Accordingly, the equilibrium radius of the bare micelle is

$$r_{\text{core}} \approx p_0^{1/3} v^{1/3} \approx p_0^{1/2} a_0^{1/2} \quad (3)$$

For our chosen system, with $N \gg n \gg 1$, the corona is much more extended than the core. The micellar corona is thus reminiscent of the corona of a star polymer.^{18,19} This has two consequences. First, as noted, the span of the intrachain micelle is dominated by the coronal contribution. Accordingly, the micellar radius is

$$r_{\text{micelle}} \approx p^{1/5} n^{3/5} b \gg r_{\text{core}} \quad (4)$$

where b is the size of the hydrophilic monomer. The second, an extra penalty term, F_{corona} , must supplement $\tilde{\epsilon}_p$ in order to allow for the crowding of the coronal loops

$$F_{\text{corona}}/kT \approx p^{1/2} \ln(r_{\text{micelle}}/r_{\text{core}}) \approx p^{1/2} \ln n \quad (5)$$

This second penalty term also opposes micellar growth. Altogether, the free energy per amphiphile incorporated into a spherical intrachain micelle, $\epsilon_p kT$, is thus $\epsilon_p \approx \tilde{\epsilon}_p + F_{\text{corona}}/kT$. Upon defining a dimensionless variable

$$u = p/p_0 = (a_0/a)^3 \quad (6)$$

we may rewrite ϵ_p as²⁰

$$\epsilon_p \approx \gamma a_0(u^{-1/3} + u^{1/3} + \kappa u^{1/2}) - \delta \quad (7)$$

Here $\kappa \approx p_0^{1/2} \ln n/\gamma a_0$ is a dimensionless parameter measuring the relative importance of F_{corona} and $\tilde{\epsilon}_p$ of the bare micelle for $a \approx a_0$.²¹ The equilibrium characteristics of the intrachain micelles are specified by the condition $\partial \epsilon_p / \partial u = 0$.¹² However, the main results are obtainable via a simpler argument. When $\kappa \ll 1$, the coronal contribution to ϵ_p , $\kappa u^{1/2}$, is negligible. In this limit, the surface energy term in ϵ_p , $u^{-1/3}$, is comparable to the head group penalty, $u^{1/3}$. Accordingly, $u \approx 1$ and the micellar characteristics in this regime are

$$a \approx a_0 \quad (8)$$

$$r_{\text{core}} \approx p_0^{1/2} a_0^{1/2} \quad (9)$$

$$r_{\text{micelle}} \approx p_0^{1/5} n^{3/5} b \quad (10)$$

Having specified the equilibrium structure of the intrachain micelles, we are now in a position to describe the configurations of a linear string of $m/p_0 \gg 1$ intrachain micelles. As noted earlier, it is assumed that all amphiphiles are assembled into micelles. The validity of this assumption is discussed in section V. The string is expected to behave as a self-avoiding chain consisting of intrachain micelles instead of monomers. The span of the chain is thus given by the appropriate Flory radius, $R_F(p) \approx (m/p)^{3/5} r_{\text{micelle}} \approx R_F u^{-2/5}$, and in the $\kappa \ll 1$ limit, we have

$$R_F \approx m^{3/5} p_0^{-2/5} n^{3/5} b \quad (11)$$

It is also useful to specify the length of a fully extended string of unperturbed micelles, $R_{\text{max}}(p) \approx (m/p) r_{\text{micelle}}$. In the $\kappa \ll 1$ case

$$R_{\text{max}} \approx m p_0^{-4/5} n^{3/5} b \approx (m/p_0)^{2/5} R_F \quad (12)$$

In the opposite limit, of $\kappa \gg 1$, the head group repulsion penalty, $u^{1/3}$, is negligible. Accordingly, the surface energy term, $u^{-1/3}$, is comparable to the coronal penalty $\kappa u^{1/2}$. The equilibrium characteristics of this case are listed in Appendix III.

III. Extension of a Uniform String of Micelles

In this section we consider the extension of a uniform string of micelles, focusing on the $\kappa \ll 1$ limit. That is, we assume that the sole effect of the extension is a decrease in the aggregation number from p_0 to p and a corresponding increase in the number of micelles from

m/p_0 to m/p . In this case, the free energy per chain, F_{chain} , reflects two contributions. First is the micellar term, $m\epsilon_p$. It allows for the free energy of the aggregated amphiphiles as p decreases below p_0 . The second contribution, F_{el} , is the elastic free energy of the string as a whole. It reflects the loss of configurational entropy upon extension.

The extension of the uniform string involves four regimes, each characterized by a different F_{el} . For weak extensions, while $R_F(u) < R \ll R_{\text{max}}(u)$, a Gaussian behavior is expected.² In this linear response regime $F_{\text{el}}/kT \approx [R/R_F(u)]^2 \approx (R/R_F)^2 u^{4/5}$. Upon further extension, when $R_F(u) \ll R \ll R_{\text{max}}(u)$, F_{el} assumes the Pincus form,^{2,22} $F_{\text{el}}/kT \approx [R/R_F(u)]^{5/2} \approx (R/R_F)^{5/2} u$. When R exceeds $R_{\text{max}}(u)$, the length of a fully extended string, a third regime comes into play. In it, the bridges between the micelles are stretched.^{9,10} m/p bridges, each consisting of n monomers, are involved. The Pincus F_{el} is applicable since the bridges are already stretched in the unperturbed state because of the coronal interactions. However, in the stretched bridges regime $R_F(u)$ should be replaced by

$$R_B(u) \approx (mn/p)^{3/5} b \approx (mn/p_0)^{3/5} u^{-3/5} b \approx R_B u^{-3/5} \quad (13)$$

where $R_B \approx (mn/p_0)^{3/5} \approx p_0^{-1/5} R_F$. Accordingly, $F_{\text{el}}/kT \approx [R/R_B(u)]^{5/2} \approx (R/R_F)^{5/2} p_0^{1/2} u^{3/2}$. Finally, when $R \gg R_{\text{max}}(u)$ and $u \approx 1/p_0$, the secondary structure no longer influences the elastic behavior since all the amphiphiles are dissociated. In this range $F_{\text{chain}}/kT \approx F_{\text{el}}/kT \approx [R/(mn)^{3/5} b]^{5/2} \approx (R/R_F)^{5/2} p_0^{-1}$. For the first three regimes F_{chain} is

$$F_{\text{chain}}/kT \approx m\gamma a_0 [u^{-1/3} + u^{1/3} + \kappa u^{1/2} + \tau(R)u^\alpha] - m\delta \quad (14)$$

where $\tau(R) \approx F_{\text{el}}(R)/m\gamma a_0$ is the ratio of the appropriate elastic free energy and $m\epsilon_p$ at $p = p_0$ and a given R . In the Gaussian regime $\tau_g \approx (m\gamma a_0)^{-1} (R/R_F)^2$ and $\alpha_g = 4/5$, while in the Pincus regime $\tau_p \approx (m\gamma a_0)^{-1} (R/R_F)^{5/2}$ and $\alpha_p = 1$. Finally, in the stretched bridges regime $\tau_b \approx (m\gamma a_0)^{-1} (R/R_F)^{5/2} p_0^{1/2}$ and $\alpha_b = 3/2$. The value of $\tau(R)$ determines the onset of significant perturbation of the micellar structure due to the elastic contribution.

F_{chain} as written above is valid for any κ . In the limit of $\kappa \ll 1$, considered at present, the coronal term, $\kappa u^{1/2}$, is negligible. Thus, the equilibrium condition for the extended chain, $\partial F_{\text{chain}}(R)/\partial u = 0$, leads to

$$u^{2/3} + \tau u^{\alpha+1/3} \approx 1 \quad (15)$$

While $\tau \ll 1$, the second term is negligible, $u \approx 1 - 3\tau/2 \approx 1$, and the micelles are only weakly perturbed. In this limit the driving term in F_{chain} , $u^{-1/3}$, is comparable to the head group penalty, $u^{1/3}$. In the opposite situation, $\tau \gg 1$, the second term is dominant and thus $u \approx \tau^{-1/(\alpha+1/3)}$. In other words, the $u^{-1/3}$ term in F_{chain} is comparable to the elastic term, τu^α . The crossover between the two regimes occurs at $R \approx R^*$ defined by $\tau(R^*) \approx 1$. As we shall see, this condition is fulfilled in the stretched bridges regime. The condition $\tau_g(R^*) \approx 1$ leads to $R^* \approx R_F(m\gamma a_0)^{1/2} \approx m^{1/10} p_0^{2/5} (\gamma a_0)^{1/2} R_{\text{max}}$, while $\tau_p(R^*) \approx 1$ yields $R^* \approx R_F(m\gamma a_0)^{2/5} \approx p_0^{2/5} (\gamma a_0)^{2/5} R_{\text{max}}$. In both cases $R^* > R_{\text{max}}$. It is also instructive to note that $\tau_g(R_{\text{max}}) \ll 1$ and $\tau_p(R_{\text{max}}) \ll 1$. In both cases R^* is outside the range of validity of the corresponding F_{el} . Thus, in these two regimes the aggregation number is only slightly reduced, i.e., $u \approx 1$. Accordingly, F_{chain} in

the Gaussian regime is

$$F_{\text{chain}}/kT \approx m\epsilon_{p_0} + (R/R_F)^2 \quad (16)$$

while in the Pincus regime

$$F_{\text{chain}}/kT \approx m\epsilon_{p_0} + (R/R_F)^{5/2} \quad (17)$$

where $\epsilon_{p_0} \approx 2\gamma a_0 - \delta$. The condition $\tau(R^*) \approx 1$ is satisfied in the stretched bridges regime where $\tau_b \approx 1$ leads to

$$R^* \approx (m\gamma a_0)^{2/5} p_0^{-1/5} R_F \approx p_0^{1/5} (\gamma a_0)^{2/5} R_{\text{max}} > R_{\text{max}} \quad (18)$$

This domain is thus split into two parts. For $R_{\text{max}} < R < R^*$, $u \approx 1$ and, accordingly,

$$F_{\text{chain}}/kT \approx m\epsilon_{p_0} + (R/R_B)^{5/2} \approx m\epsilon_{p_0} + (R/R_F)^{5/2} p_0^{1/2} \quad (19)$$

On the other hand, for $R^* < R < R_{**}$, we obtain $u \approx \tau_b^{-6/11} \ll 1$, thus leading to $F_{\text{chain}}/kT \approx m\gamma a_0 \tau_b^{2/11} - m\delta$ or

$$F_{\text{chain}}/kT \approx (m\gamma a_0)^{9/11} (R/R_F)^{5/11} p_0^{1/11} - m\delta \quad (20)$$

The upper boundary of this regime, R_{**} , is determined by setting $u \approx \tau_b^{-6/11}$ equal to p_0^{-1} , thus yielding

$$R_{**} \approx (m\gamma a_0)^{2/5} p_0^{8/15} R_F \approx p_0^{11/15} R^* \quad (21)$$

As was noted previously, for $R > R_{**}$ the polysoap is fully dissociated and

$$F_{\text{chain}}/kT \approx p_0^{-1} (R/R_F)^{5/2} \quad (22)$$

Having obtained F_{chain} for the full range of chain extensions we are now in a position to specify the tension along the chain, $f = \partial F_{\text{chain}}/\partial R$, in the various regimes.

$$\begin{aligned} f/kT &\approx R/R_F^2 \sim R & R_F < R \ll R_{\text{max}} \\ f/kT &\approx R^{3/2}/R_F^{5/2} \sim R^{3/2} & R_F \ll R \ll R_{\text{max}} \\ f/kT &\approx R^{3/2} p_0^{1/2}/R_F^{5/2} \sim R^{3/2} & R_{\text{max}} \ll R < R^* \\ f/kT &\approx (m\gamma a_0)^{9/11} p_0^{1/11}/R^{6/11} R_F^{5/11} \sim R^{-6/11} & R^* < R < R_{**} \\ f/kT &\approx R^{3/2}/p_0 R_F^{5/2} \sim R^{3/2} & R_{**} < R \end{aligned} \quad (23)$$

The sequence of force laws listed above reveals two notable features (Figure 3): (i) The tension in the chain changes abruptly at the boundary between the Pincus and stretched bridges regimes. At the upper boundary of the Pincus regime the tension is $f(R_{\text{max}} - 0) \approx (R_{\text{max}}/R_F)^{3/2} R_F^{-1} \approx 1/\ell_{\text{micelle}}$, while at the lower boundary of the stretched bridges regime it is $f(R_{\text{max}} + 0) \approx (R_{\text{max}}/R_F)^{3/2} p_0^{1/2} R_F^{-1} \approx p_0^{1/2}/\ell_{\text{micelle}} \approx 1/\xi_0$, where ξ_0 is the size of the outermost blob in the micellar corona (Appendix I). Thus $f(R_{\text{max}} - 0)/f(R_{\text{max}} + 0) \approx 1/p_0^{1/2}$. This jump occurs because the unperturbed bridges are already stretched due to the crowding of the coronal loops. (ii) More importantly, the fR diagram displays a van der Waals loop. f increases with R up to a value of $f^* \approx (\gamma a_0 p_0/n)^{3/5}$ attained at R^* . Between R^* and R_{**} the tension decreases as $f \sim R^{-6/11}$. Eventually, for $R > R_{**}$,

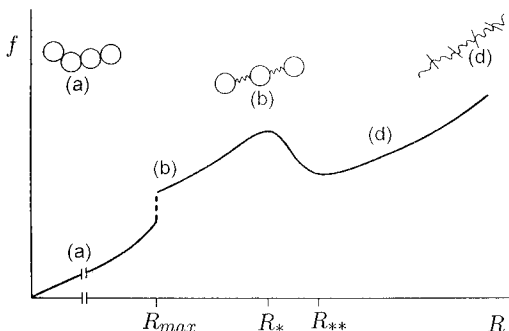


Figure 3. fR diagram exhibiting a van der Waals loop due to the assumption that chain extension results only in repartitioning of amphiphiles among intrachain micelles of uniform size.

the tension grows again as $f \sim R^{3/2}$. The van der Waals loop indicates that the effect of the tension is not limited to a uniform reduction of the aggregation number, as was assumed. It suggests that at intermediate extensions, weakly perturbed micelles coexist with fully dissociated amphiphiles.

IV. Extension with Coexistence

In the preceding section it was assumed that the extension of the polysoap leads only to the rearrangement of the amphiphiles within the micelles, *i.e.*, to a uniform decrease in the aggregation number with a corresponding increase in the number of micelles. The fR diagram derived on this basis displays a van der Waals loop, indicating that this assumption is not valid over the full range of extensions. It suggests that at intermediate extensions weakly perturbed micelles coexist with fully dissociated amphiphiles. No modifications are expected for weak extensions. Similarly, the strong extension regime, $R^* < R$, is also expected to survive. The initial discussion, in this section, will ignore the role of S_{mix} , the mixing entropy of the one-dimensional solution of micelles and dissociated amphiphiles. As a result, the fR diagram exhibits features of a first-order phase transition. Most notable is a sharply defined plateau characterized by $f \sim R^0$. As we shall see, allowing for S_{mix} will smooth the crossovers to the adjacent regimes and introduce a logarithmic R dependence in f . The role of S_{mix} and the resulting modifications will be discussed in the next section.

In the coexistence regime, an extra degree of freedom comes into play, $0 < \psi < 1$, the fraction of amphiphiles incorporated into micelles. ψm amphiphiles will form weakly perturbed intrachain micelles, while the remaining $(1 - \psi)m$ will be dissociated. In the following we limit the discussion to the case of $\kappa \ll 1$. The modifications required for the $\kappa \gg 1$ limit will be discussed briefly in Appendix III. Since the onset of coexistence is expected to occur at $R_L \ll R^*$, so that $\tau(R_L) \ll 1$, we neglect the weak perturbation of the micellar structure. In particular, it is assumed that $p \approx p_0$. We first analyze the coexistence regime using a $T = \text{const}'$, $R = \text{const}'$ ensemble. This adapts our earlier results^{9,10} to the case of a good solvent for the hydrophilic backbone. Later we reconsider the problem by utilizing a $T = \text{const}'$, $f = \text{const}'$ ensemble. Since S_{mix} is presently ignored, the free energy of the chain consists of two terms. First is the micellar term

$$F_{\text{micelle}}/kT \approx m\psi\epsilon_{p_0} \quad (24)$$

This term allows for the free energy of amphiphiles

incorporated into micelles. For $\kappa \approx 1$, when $p \approx p_0$, $\epsilon_p \approx \epsilon_{p_0}$ is related to X_{cmc} , the critical micelle concentration of the free, unpolymerized, amphiphiles, as $\epsilon_{p_0} \approx \ln X_{\text{cmc}}$. The micellar term is supplemented by a term allowing for the elasticity of the chain, F_{el} . This assumes two different forms for the two regimes of interest. In the Pincus regime

$$F_{\text{el}}/kT \approx [R/R_F(\psi)]^{5/2} \quad (25)$$

where

$$R_F(\psi) \approx (mn)^{3/5} b[p_0^{-2/3}\psi + (1 - \psi)]^{3/5} \approx R_F[\psi(1 - p_0^{2/3}) + p_0^{2/3}]^{3/5} \quad (26)$$

is the Flory radius of the partially dissociated chain (Appendix II) and $R_F/b \approx m^{3/5}r^{3/5}p_0^{-2/5}$ is the Flory radius of the unperturbed string. It is important to note that this is an underestimate of $R_F(\psi)$. In this approximation $R_F(\psi)$ is dominated by the contribution of the dissociated chain segments because each dissociated micelle “releases” pn monomers. To obtain the proper crossover behavior at $\psi = 1$, this form also allows for the smaller contribution due to micelle–micelle interactions. However, the effect of micelle–monomer interactions is neglected. In the stretched bridges regime

$$F_{\text{el}}/kT \approx [R/R_B(\psi)]^{5/2} \quad (27)$$

where

$$R_B(\psi)/b \approx (mn)^{3/5} [(1 - \psi) + p_0^{-1}\psi]^{3/5} \approx R_B[p_0 + (1 - p_0)\psi]^{3/5} \quad (28)$$

and $R_B \approx (mn/p_0)^{3/5}$.

As we shall see, the onset of coexistence occurs at the stretched bridges regime, for $R_L > R_{\text{max}}$. Assuming that it occurs in the Pincus range leads to inconsistencies, *i.e.*, $R_L > R_{\text{max}}$. In the stretched bridges regime

$$F_{\text{chain}}/kT \approx m\psi\epsilon_{p_0} + (R/R_B)^{5/2} [\psi(1 - p_0) + p_0]^{-3/2} \quad (29)$$

As noted earlier, in the approximation scheme invoked in this section we omit a third term, $-S_{\text{mix}}/k$, from F_{chain}/kT . The equilibrium state of a chain, for a given R , is specified by $\partial F_{\text{chain}}/\partial \psi = 0$, leading to

$$\psi \approx p_0/(p_0 - 1) - (R/R_B)(m|\epsilon_{p_0}|)^{-2/5}(p_0 - 1)^{-3/5} \quad (30)$$

This reduces to $\psi \approx 1 - (R/R_B)(m|\epsilon_{p_0}|)^{-2/5}p_0^{-3/5}$ in the limit of $p_0 \gg 1$. However, retaining the more general form is important for the precise determination of the boundaries of the coexistence regime. Upon substituting this expression for ψ in F_{chain} , as given by (29), we obtain $F_{\text{chain}}(R)$ in the limit of $p_0 \gg 1$

$$F_{\text{chain}}/kT \approx -m|\epsilon_{p_0}| + (R/R_B)(m|\epsilon_{p_0}|/p_0)^{3/5} \quad (31)$$

The force at coexistence, f_{co} , in this limit is thus

$$f_{\text{co}}/kT \approx (1/R_B)(m|\epsilon_{p_0}|/p_0)^{3/5} \approx |\epsilon_{p_0}|^{3/5}/n^{3/5}b \quad (32)$$

Accordingly, the assumption of coexistence and the corresponding free energy lead to the replacement of the van der Waals loop by a plateau (Figure 4). The upper and lower boundaries of the coexistence region, R_L and R_U , can be determined in two ways: first, by matching

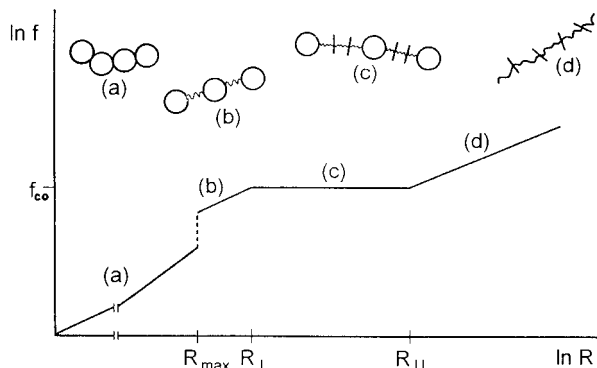


Figure 4. fR diagram with a plateau, $f \sim R^3$, replacing the van der Waals loop, occurring when a coexistence between weakly perturbed intrachain micelles and fully dissociated amphiphiles is allowed.

f_{co} with the tension in the neighboring regimes; second, via the conditions $\psi(R_L) = 1$ and $\psi(R_U) = 0$. The condition $\psi(R_L) = 1$ yields

$$R_L \approx [m|\epsilon_{p_0}|/(p_0 - 1)]^{2/5} R_B \approx |\epsilon_{p_0}|^{2/5} m n^{3/5} / p_0 \approx |\epsilon_{p_0}|^{2/5} p_0^{-1/5} R_{max} < R_* \quad (33)$$

The same result is obtained if R_L is assumed to occur within the stretched bridges regime, upon equating f_{co} to $R_L^{3/2}/R_B^{5/2}$. Note that $R_L > R_{max}$, as required by the assumption that the onset of coexistence occurs at the stretched bridges regime. This is because the stability condition of the intrachain micelles imposes $|\epsilon_{p_0}| > p_0^{1/2}$. To determine R_U , we use $f_{co}/kT \approx R_U^{3/2}/p_0 R_F^{5/2}$, leading to

$$R_U \approx |\epsilon_{p_0}|^{2/5} m n^{3/5} b \approx |\epsilon_{p_0}|^{2/5} p_0^{4/5} R_{max} > R_* \quad (34)$$

The same result is obtained by invoking $\psi(R_U) \approx 0$.

Having obtained the coexistence curve, it is instructive to consider the problem using a different approach. In the preceding discussion, the equilibrium condition $\partial F_{chain}/\partial \psi = 0$ was stated for constant T and R , assuming that $p \approx p_0$. This condition specifies $\psi = \psi(R)$ at equilibrium and thus yields $F_{chain}(R)$ and the corresponding tension, $f = \partial F_{chain}/\partial R$. Pursuing this route requires explicit expressions for $R_B(\psi)$ and for $R_F(\psi)$. In turn, this leads to cumbersome equations and requires the introduction of approximate forms for $R_F(\psi)$ and $R_B(\psi)$. A simpler analysis, free of these approximations, is possible since the tension at coexistence is expected to be constant, $f = f_{co}$. It is thus appropriate to analyze the equilibrium behavior for constant T and f . The corresponding equilibrium condition as stated in terms of $G_{chain}(\psi, R) = F_{micelle} + F_{el} - fR$ is $dG_{chain} = (\partial G_{chain}/\partial \psi)d\psi + (\partial G_{chain}/\partial R)dR = 0$. The requirement $\partial G_{chain}/\partial \psi = 0$ is equivalent to $\partial F_{chain}/\partial \psi = 0$, while $\partial G_{chain}/\partial R = 0$ sets the R corresponding to the imposed f . At coexistence, f does not specify a unique R . Rather, $f = f_{co}$ for any $R_L < R < R_U$. For this range we may thus substitute f as given by $(\partial G_{chain}/\partial R) = 0$ into G_{chain} , obtaining

$$dG_{chain}/kT = -m|\epsilon_{p_0}|d\psi - (f_{co}/kT)dR = 0 \quad (35)$$

This condition can be reformulated in terms of $\Delta G_{chain} = G_{chain}(R) - G_{chain}(R_L)$, $\Delta G_{chain}/kT \approx m|\epsilon_{p_0}|(1 - \psi) - (f_{co}/kT)(R - R_L)$. It states that the two terms in $\Delta G_{chain}/kT$ are comparable. In turn, (35) leads to

$$d\psi/dR \approx -f_{co}/kTm|\epsilon_{p_0}| \quad (36)$$

Integration of (36), together with the condition $\psi(R_U) = 0$, yields $\psi \approx (f_{co}/kTm|\epsilon_{p_0}|)(R_U - R)$, and by invoking $\psi(R_L) = 1$, we obtain

$$f_{co}/kT = m|\epsilon_{p_0}|/(R_U - R_L) \quad (37)$$

and

$$\psi \approx (R_U - R)/(R_U - R_L) \quad (38)$$

These two expressions are equivalent to (30) and (32) obtained above. Note also that (38) leads to $1 - \psi = (R - R_L)/(R_U - R_L)$ and thus to

$$\psi/(1 - \psi) \approx (R_U - R)/(R - R_L) \quad (39)$$

This last expression is the lever rule¹⁴ for our system. It determines the relative amounts of the two "phases" in terms of the position of the system on the coexistence curve. Note further that the $p_0 \gg 1$ limit corresponds, in these terms, to the case of $R_U \gg R_L$. To obtain the explicit expressions for f_{co} , R_L , and R_U , we utilize the following three conditions $f_{co}/kT \approx R_U^{3/2}/p_0 R_F^{5/2} \approx R_L^{3/2}/R_B^{5/2}$. These lead to

$$R_U \approx p_0 R_L \quad (40)$$

to

$$R_L \approx [m|\epsilon_{p_0}|/(p_0 - 1)]^{2/5} R_B \quad (41)$$

and, finally, to

$$f_{co}/kT \approx m|\epsilon_{p_0}|/(p_0 - 1)R_L \approx [m|\epsilon_{p_0}|/(p_0 - 1)]^{3/5} R_B^{-1} \quad (42)$$

Altogether, this second derivation allows us to recover all the results obtained previously. It thus justifies the approximations used earlier for $R_F(\psi)$ and for $R_B(\psi)$. As an extra benefit, it naturally leads to expressions for ψ and f_{co} in terms of R_L and R_U , thus yielding the lever rule for this system.

V. Extension with Coexistence: Effect of the Mixing Entropy

The analysis presented in section IV ignores the role of the one-dimensional mixing entropy. In effect, the micelles and the dissociated amphiphiles are assumed to segregate. This approximation, while convenient and useful, oversimplifies the situation. In the stretched bridges regime there can be no bridging attraction between micelles. Accordingly, dissociated amphiphiles and micelles are expected to be randomly dispersed. It is thus necessary to supplement F_{chain} , as given by (29), with a term accounting for the associated mixing entropy, $S_{mix}(\psi)$. As we shall see, this term will modify the fR diagram in two respects: (i) The force now increases logarithmically with R instead of $f \sim R^3$. (ii) The sharp boundaries of the coexistence regime are replaced by smooth crossover regions. In addition $S_{mix}(\psi)$ gives rise to an upper bound on m , m_u , above which the assumption that the nonextended chain is fully micellized becomes untenable.

To proceed, it is first necessary to obtain an explicit form for $S_{mix}(\psi)$. This requires a certain care. Clearly, calculating $S_{mix}(\psi)$ involves the inscription of micelles

and dissociated amphiphiles on a one-dimensional lattice with a lattice constant defined by the spacer chains. However, the total number of sites *varies* with ψ . To allow for this feature, it is helpful to formulate the problem in terms of junctions involving "noncoronal" spacers, *i.e.*, spacers that join two micelles, two dissociated amphiphiles, or a dissociated amphiphile and a micelle. A polysoap incorporating m amphiphiles consists of $m - 1$ spacers. Each of the $\psi m/p_0$ micelles incorporates $p_0 - 1$ coronal spacers. The number of noncoronal spacers is thus $m - 1 - (p_0 - 1)\psi m/p_0$. The number of junctions, $M\psi$, is greater by 1, that is $M_\psi = m(1 - \psi) + \psi m/p_0$. Each junction can be either a micelle or an amphiphile. The number of possibilities of choosing $\psi m/p_0$ junctions to be micelles is

$$W = [m(1 - \psi) + \psi m/p_0]! / (\psi m/p_0)! [m(1 - \psi)]! \quad (43)$$

The entropy, $S_{\text{mix}}k = \ln W$, as obtained by invoking the Stirling approximation, is

$$S_{\text{mix}}/mk = (1 - \psi) \ln \left[\frac{p_0(1 - \psi) + \psi}{p_0(1 - \psi)} \right] + \frac{\psi}{p_0} \ln \left[\frac{\psi + (1 - \psi)p_0}{\psi} \right] \quad (44)$$

For $\psi \ll 1$ this leads to $S_{\text{mix}}/mk \approx -(\psi/p_0) \ln(\psi/p_0)$, while for $\psi \approx 1$, $S_{\text{mix}}/mk \approx -(1 - \psi) \ln p_0(1 - \psi)$. $S_{\text{mix}} = dS_{\text{mix}}/d\psi$ will play an important role in our subsequent discussion.

$$S_{\text{mix}}/mk = -\ln \left[\frac{p_0(1 - \psi) + \psi}{p_0(1 - \psi)} \right] + \frac{1}{p_0} \ln \left[\frac{\psi + (1 - \psi)p_0}{\psi} \right] \quad (45)$$

For $\psi \approx 1$, $S_{\text{mix}}/mk \approx \ln p_0(1 - \psi)$, whereas for $\psi \ll 1$, $S_{\text{mix}}/mk \approx p_0^{-1} \ln p_0/\psi$. S_{mix} vanishes at ψ_0 . By assuming, and later verifying, that $[1 + \psi_0/p_0(1 - \psi_0)]^{p_0} \approx 1 + \psi_0/(1 - \psi_0)$ we obtain

$$\psi_0 \approx 1 - p_0^{-1/2} \quad (46)$$

It is convenient to begin the discussion with the free energy of an unperturbed polysoap

$$F_{\text{chain}}/kT \approx m\psi\epsilon_{p_0} - S_{\text{mix}}/k \quad (47)$$

This free energy describes the possible coexistence of two "phases", micellized and dissociated, in a one-dimensional system experiencing short-range interactions. In the limit of an infinite system, the coexisting phases cannot be arbitrarily large because of S_{mix} .¹⁴ In our case, however, the system is of finite length. Here, F_{chain} sets the limits of validity of our initial assumption that all amphiphiles in the unperturbed polysoap self-assemble into micelles. As we shall see, this assumption is tenable only up to a maximal $m = m_u$ to be specified later. For $m > m_u$, micellized and dissociated amphiphiles must coexist, even in the absence of an externally applied tension. To specify m_u , it is helpful to consider F_{chain} in the vicinity of $\psi = 1$. In this regime

$$F_{\text{chain}}/kT \approx F_0/kT + m|\epsilon_{p_0}|(1 - \psi) + m(1 - \psi) \ln p_0(1 - \psi) \quad (48)$$

where $F_0/kT = m\epsilon_{p_0}$. This free energy represents a one-dimensional solution of dissociated amphiphiles dispersed in a string of micelles. $\partial F_{\text{chain}}/\partial\psi \rightarrow \infty$ as $\psi \rightarrow 1$, thus indicating that ψ should decrease so as to lower F_{chain} . The equilibrium value of ψ for a chain comprising m amphiphiles is related to the average number of dissociated micelles, n_d , as $\psi \approx 1 - n_d p_0/m$. The equilibrium value is specified by $\partial F_{\text{chain}}/\partial\psi = 0$, leading to $\ln(n_d p_0^2/m) + |\epsilon_{p_0}| \approx 0$ or to

$$m p_0^{-2} \exp(-|\epsilon_{p_0}|) \approx n_d \quad (49)$$

The condition $n_d = 1$ determines m_u , when the chain supports, on average, a single dissociated micelle

$$m_u \approx p_0^2 \exp(|\epsilon_{p_0}|) \quad (50)$$

Accordingly, the average number of dissociated micelles per chain is

$$n_d \approx m/m_u \quad (51a)$$

Notice that this sets an upper limit on ψ

$$\bar{\psi} \approx 1 - p_0/m_u \approx 1 - p_0^{-1} \exp(-|\epsilon_{p_0}|) \quad (51b)$$

Notice further that $m_u \gg p_0^2$ since $\exp(-|\epsilon_{p_0}|) \approx X_{\text{cmc}} \ll 1$, where X_{cmc} is the critical micelle concentration of the unpolymerized amphiphiles. The analysis presented in the following is limited to the case $m \ll m_u$. For such m , the fraction of chains supporting dissociated micelles is negligible and we may assume that the unperturbed chains are fully micellized. Since $m_u \gg p_0^2$, this is a realistic scenario.

With this in mind we are in a position to analyze $F_{\text{chain}}(R, \psi)$ at coexistence

$$F_{\text{chain}}/kT \approx m\psi\epsilon_{p_0} + (R/R_B)^{5/2} [\psi(1 - p_0) + p_0]^{-3/2} - S_{\text{mix}}/k \quad (52)$$

The elastic term may be viewed as an external field favoring the dissociated "phase". An increase in f , or in the imposed R , always favors a decrease in ψ . On the other hand, S_{mix} always favors intermediate values of ψ . It thus lowers $\tilde{f}_{\text{co}}/\tilde{f}_{\text{co}}$ in the vicinity of $\psi = 1$, while increasing it in the neighborhood of $\psi = 0$. Within this approach it is impossible to solve for $\tilde{f}_{\text{co}} = \tilde{f}_{\text{co}}(R)$ explicitly. Instead, we can obtain a parametric solution $\tilde{f}_{\text{co}} = \tilde{f}_{\text{co}}(\psi)$. In particular, we solve for the equilibrium values of $\tilde{R} = \tilde{R}(\psi)$ and of $\tilde{f} = \tilde{f}(\psi)$. Here the tilde is used to distinguish the equilibrium values obtained when allowing for S_{mix} from those obtained in the previous section. The corresponding fR diagram is found numerically. The condition $\partial F_{\text{chain}}/\partial\psi = 0$ yields

$$\tilde{R} \approx R_B [m|\epsilon_{p_0}| + S_{\text{mix}}/k]^{2/5} [\psi(1 - p_0) + p_0]/(p_0 - 1)^{2/5} \quad (53)$$

Upon substituting this \tilde{R} into (52), we obtain $F_{\text{chain}}(\psi)$ in equilibrium. The force at coexistence, as a function of ψ , is $\tilde{f}_{\text{co}} = dF_{\text{chain}}(\psi)/dR = (dF_{\text{chain}}/d\psi)(dR/d\psi)^{-1}$ or

$$\tilde{f}_{\text{co}} \approx \tilde{f}_{\text{co}}(1 + S_{\text{mix}}/km|\epsilon_{p_0}|)^{3/5} \quad (54)$$

where \tilde{f}_{co} is the tension at coexistence as given by (32), when S_{mix} is neglected. For $0 \ll \psi \ll 1$ the fR diagram now exhibits a logarithmic correction to $\tilde{f}_{\text{co}} \sim R^0$. \tilde{f}_{co}

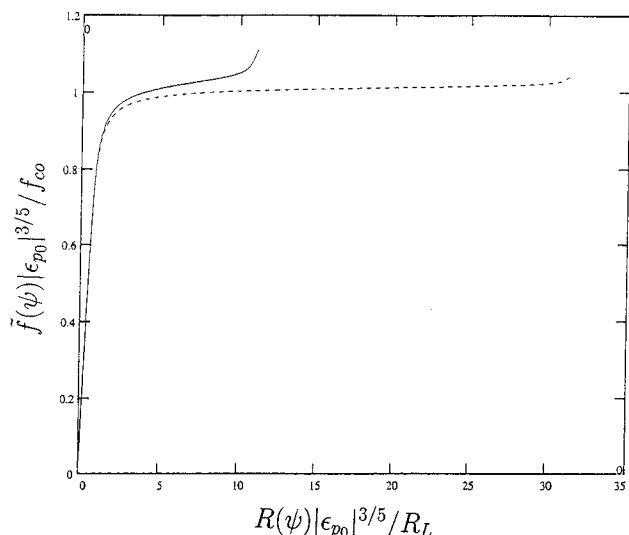


Figure 5. Plot of $\tilde{f}(\psi)|\epsilon_{p0}|^{3/5}/f_{co}$ vs $\tilde{R}(\psi)|\epsilon_{p0}|^{1/2}/R_L$ for $|\epsilon_{p0}| = 10$ (continuous line) and for $|\epsilon_{p0}| = 30$ (broken line).

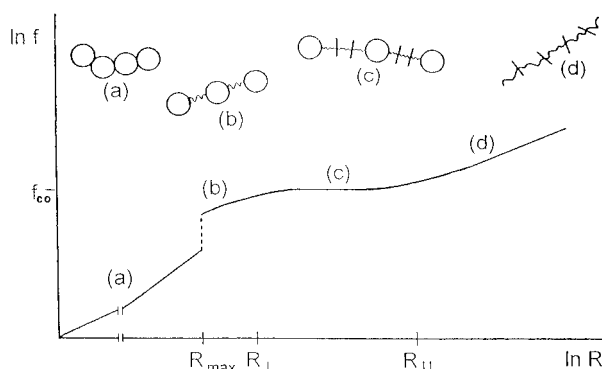


Figure 6. Schematic fR diagram incorporating $\tilde{f}_{co}(R)$ and thus allowing for the role of S_{mix} . Note the smooth crossovers and the weakly increasing \tilde{f}_{co} .

increases weakly with R . S_{mix} is negligible in the vicinity of ψ_0 and the corresponding $\tilde{R}(\psi_0) \approx p_0^{1/2}R_L$. Consequently, in this region it is possible to replace (53) by (39) obtained in section IV. By substituting (39) into (45), it is possible to approximate \tilde{f}_{co} in this region by

$$\tilde{f}_{co} \approx f_{co}(1 + \ln g(R)/|\epsilon_{p0}|)^{3/5} \quad (55)$$

where $g(R)$ is a slowly increasing function of R

$$g(R) \approx \left[1 + \frac{1}{p_0} \left(\frac{R_U - R}{R - R_L} \right) \right] \left[1 + p_0 \left(\frac{R - R_L}{R_U - R} \right) \right]^{1/p_0} \quad (56)$$

These logarithmic corrections become important in the immediate neighborhood of $\psi = 1$ and $\psi = 0$ where the above approximation is no longer valid (Figure 5). To obtain the upper and lower boundaries of the coexistence regime, \tilde{R}_U and \tilde{R}_L , it is necessary to carefully specify the corresponding values of ψ . As was stated earlier, it is assumed that prior to the onset of coexistence all amphiphiles are assembled into micelles. In the coexistence regime, we further assume that fully dissociated amphiphiles coexist with weakly perturbed micelles. Within this approximation, the lower and upper boundaries of the coexistence regime correspond, respectively, to chains supporting one dissociated micelle and to chains supporting one undissociated micelle. In other words, the maximal and minimal values of ψ at coexistence are respectively $\psi_{max} \approx 1 - p_0/m$ and ψ_{min}

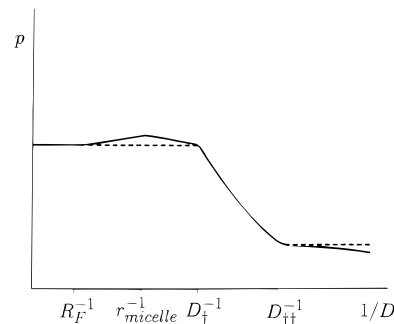


Figure 7. Nonmonotonic variation in the aggregation number of the intrachain micelles upon confinement. The weak initial increase reflects the response to the chain confinement. The subsequent development is dominated by the coronal contribution.

$\approx p_0/m$. Within the $S_{mix} = 0$ approximation it was possible to consider arbitrarily large m and thus to set $\psi_{max} \approx 1$ and $\psi_{min} \approx 0$. In our case, however, we are limited to $m \ll m_u$ and this is no longer possible. To obtain \tilde{R}_L and \tilde{R}_U , we use $\tilde{f}(\psi_{max})/kT \approx R_L^{3/2}/R_B^{5/2}$ and $\tilde{f}(\psi_{min})/kT \approx \tilde{R}_U^{3/2}/p_0 R_F^{5/2}$. These lead to $\tilde{R}_L \approx R_L[1 + S_{mix}(\psi_{max})/km|\epsilon_{p0}|^{2/5}]$ and to $\tilde{R}_U \approx R_U[1 + S_{mix}(\psi_{min})/km|\epsilon_{p0}|^{2/5}]$, where $R_L \approx R_B^{5/3}(f_{co}/kT)^{2/3}$ and $R_U \approx p_0^{2/3}R_F^{5/3}$. $(f_{co}/kT)^{2/3}$ are the lower and upper boundaries as specified by (33) and (34) (Figure 6). Altogether

$$\tilde{R}_L \approx R_L \left[1 + \frac{\ln(p_0^2/m)}{|\epsilon_{p0}|} \right]^{2/5} \quad (57)$$

$$\tilde{R}_U \approx R_U \left[1 + \frac{\ln m}{p_0|\epsilon_{p0}|} \right]^{2/5} \quad (58)$$

Note that both $\tilde{f}_{co}(\psi_{max})$ and \tilde{R}_L decrease as m increases and vanish when $\ln(p_0^2/m) + |\epsilon_{p0}| = 0$. In particular, both $\tilde{f}_{co}(\psi_{max})$ and \tilde{R}_L vanish as $|\epsilon_{p0}|^{-1} \ln(m/m_u)$ when $m \rightarrow m_u$. This is due to the growing importance of S_{mix} in destabilizing the micelles in the unperturbed chain. However, as noted before, our analysis as presented above is strictly applicable to the limit of $m \ll m_u$. The study of the extension behavior for $m \approx m_u$ is beyond the scope of this paper. Finally, it is useful to note that for the realistic case of $m \ll m_u$ the $S_{mix} = 0$ approximation yields the essential features of the fR diagram. f_{co} , R_L , and R_U serve as good approximations for \tilde{f}_{co} , \tilde{R}_L , and \tilde{R}_U .

VI. Confinement to a Slit

Confinement of a linear string to a slit of width D results in rearrangement of the amphiphiles within the micelles. In marked distinction to the extension scenario there is no coexistence regime for confinement in the range $R_F > D > r_{core}$. However, as we shall see, the variation of the aggregation number is nonmonotonic (Figure 7). Initially, p is weakly increasing. For stronger deformations we expect a steep decrease, followed, essentially, by a plateau. Our analysis of the confinement behavior follows the lines of the discussion presented in section III. The free energy of the chain, F_{chain} , reflects two contributions: The micellar contribution, $m\epsilon_p$, allows for the free energy of the aggregated amphiphiles as p varies with D . The second contribution, the confinement free energy, F_{conf} , accounts for two effects: (i) In the range $R_F > D > r_{micelle}$, F_{conf} allows for the loss of configurational entropy of the string as a whole. (ii) For stronger confinement, $r_{micelle} > D > r_{core}$,

F_{conf} also allows for the free energy penalty associated with the confinement of the micellar coronas.

We may distinguish between two main regimes depending on the relative magnitude of D and r_{micelle} . While $R_F > D > r_{\text{micelle}}$, F_{conf} reflects primarily the increase in the configurational free energy of the string of micelles. As we shall see, the structure of the intrachain micelles is only weakly perturbed in this regime. Within it we can further distinguish between two ranges. Weak confinement, $R_F(u) > D \gg r_{\text{micelle}}(u)$ is associated with a "Gaussian" penalty $F_{\text{conf}}/kT \approx [R_F(u)/D]^2 \approx (R_F/D)^2 u^{-4/5}$. For stronger confinement, $R_F(u) \gg D > r_{\text{micelle}}(u)$, F_{conf} adopts the Daoud-de Gennes form,²³ $F_{\text{conf}}/kT \approx [R_F(u)/D]^{5/3} \approx (R_F/D)^{5/3} u^{-2/3}$. Altogether

$$F_{\text{chain}}/kT \approx m\gamma a_0 [u^{1/3} + u^{-1/3} + \kappa u^{1/2} + \tau u^\alpha] - m\delta \quad (59)$$

where $\tau(D) \approx F_{\text{conf}}(D)/m\gamma a_0$ is the ratio of the confinement penalty of the string and $m\tilde{\epsilon}_{p_0}$ at $p = p_0$ and a given D . In the Gaussian range $R_F(u) > D \gg r_{\text{micelle}}(u)$ and $\tau_g \approx (m\gamma a_0)^{-1}(R_F/D)^2$, $\alpha_g = -4/5$. For $R_F(u) \gg D > r_{\text{micelle}}(u)$, the Daoud-de Gennes regime, $\tau_{\text{DdG}} \approx (m\gamma a_0)^{-1}(R_F/D)^{5/3}$ and $\alpha_{\text{DdG}} = -2/3$. While D is in the range $R_F > D > r_{\text{micelle}}$ the equilibrium condition, $\partial F_{\text{chain}}/\partial u = 0$, is

$$u^{2/3} + \kappa u^{5/6} - \tau u^{\alpha+1/3} \approx 1 \quad (60)$$

In the limit of $\kappa \ll 1$ the second term is negligible. The confinement free energy gives rise to a significant perturbation of the micellar structure for D small enough to ensure that $\tau(D) > 1$. It is straightforward to check that for $D > r_{\text{micelle}}$, $\tau(D) < 1$ for both the Gaussian and for the Daoud-de Gennes regimes. Altogether, the micellar structure is only weakly perturbed, $u \approx 1 + 3\tau/2 \approx 1$, in the range $R_F > D > r_{\text{micelle}}$. The weak increase of u may be rationalized in terms of the LeChatelier principle. It results in a smaller Flory radius and thus in a weaker elastic penalty. In the Gaussian regime

$$F_{\text{chain}}/kT \approx m\epsilon_{p_0} + (R_F/D)^2 \quad (61)$$

while in the Daoud-de Gennes range

$$F_{\text{chain}}/kT \approx m\epsilon_{p_0} + (R_F/D)^{5/3} \quad (62)$$

Upon further compression, for $D < r_{\text{micelle}}(u)$, the Daoud-de Gennes contribution changes its form and becomes simply kT per micelle. This is because the micelles are the effective monomers of the string and in this regime they set the minimal size of the confinement blobs.²³ The corresponding term is $F_{\text{conf}}/kT \approx m/p \approx (m/p_0)u^{-1}$. This term is now supplemented by a coronal contribution, F_{corona} , reflecting the penalty due to the confinement of the micellar corona. While $r_{\text{micelle}}(u) > D > (n/p)^{3/5}b$, the weak confinement of the micellar coronas gives rise to a penalty of $F_{\text{corona}}/kT \approx p_0^{1/2} (r_{\text{micelle}}/D)^{5/8} u^{5/8} \approx p_0^{5/8} r^{3/8} (b/D)^{5/8} u^{5/8}$ per amphiphile (Appendix I). In this regime

$$F_{\text{chain}}/kT \approx m\gamma a_0 [u^{1/3} + u^{-1/3} + \kappa u^{1/2} + (p_0\gamma a_0)^{-1}u^{-1} + t_{\text{wc}}u^{5/8}] - m\delta \quad (63)$$

where $t_{\text{wc}} \approx (\gamma a_0)^{-1}p_0^{1/2}(r_{\text{micelle}}/D)^{5/8}$ is the ratio of the weak coronal penalty of the micelles and $m\tilde{\epsilon}_{p_0}$ at $p = p_0$ and a given D . The corresponding equilibrium condition

is

$$u^{2/3} + \kappa u^{5/6} - (p_0\gamma a_0)^{-1}u^{-2/3} + t_{\text{wc}}u^{23/24} \approx 1 \quad (64)$$

The weak confinement of the corona becomes important for $D < D_\dagger$ where D_\dagger is defined by $t_{\text{wc}}(D_\dagger) \approx 1$, leading to

$$D_\dagger \approx (p_0^{1/2}/\gamma a_0)^{8/5} r_{\text{micelle}} \sim \kappa^{8/5} \quad (65)$$

In the limit of $\kappa \ll 1$, clearly $D_\dagger \ll r_{\text{micelle}}$. While $D \gg D_\dagger$, $t_{\text{wc}} \ll 1$ and thus $u \approx 1 - 3t_{\text{wc}}/2 \approx 1$. The micellar structure is only weakly perturbed and, accordingly,

$$F_{\text{chain}}/kT \approx m\epsilon_{p_0} + mp_0^{1/2}(r_{\text{micelle}}/D)^{5/8} \quad (66)$$

As we shall demonstrate later, the string confinement penalty is still negligible in the $D_\dagger > D > (n/p)^{3/5}b$ range. However, in this regime, the coronal confinement term is dominant, leading to $u \approx t_{\text{wc}}^{-24/23}$, i.e., the surface term in eq 63, $u^{-1/3}$, is comparable to the coronal confinement penalty, $t_{\text{wc}}u^{5/8}$. Accordingly

$$u \approx (\gamma a_0)^{24/23} p_0^{-15/23} n^{-9/23} (D/b)^{15/23} \sim \kappa^{-24/23} (D/r_{\text{micelle}})^{15/23} \quad (67)$$

In turn, this leads to $F_{\text{chain}}/kT \approx m\gamma a_0 t_{\text{wc}}^{8/23}$ or

$$F_{\text{chain}}/kT \approx m\gamma a_0 (\ln n/\kappa)^{8/23} (r_{\text{micelle}}/D)^{5/23} \quad (68)$$

The lower boundary of this domain, $D_{\dagger\dagger}$, is specified by the combination of $D_{\dagger\dagger} \approx (n/p)^{3/5}b$ and $p \approx p_0 u(D_{\dagger\dagger})$ leading to

$$D_{\dagger\dagger} \approx (\gamma a_0)^{-9/20} p_0^{-3/20} n^{3/5} b \sim p_0^{-23/40} \kappa^{9/20} r_{\text{micelle}} \quad (69)$$

Note that the string confinement contribution is indeed negligible throughout this range since $(p_0 m\gamma a_0)^{-1}u^{-1}$ at $D \approx D_{\dagger\dagger}$ scales as $p_0^{-1/2}(\gamma a_0)^{-21/23} \ll 1$. The existence of this regime depends on the fulfillment of $\kappa > \ln n/p_0^{1/2}$ or $p_0 > \gamma a_0$ that ensures $D_{\dagger\dagger} < D_\dagger$,

$$D_{\dagger\dagger}/D_\dagger \approx (p_0^{1/2}/\kappa \ln n)^{-23/20} < 1 \quad (70)$$

The aggregation number at $D_{\dagger\dagger}$ is specified by

$$u(D_{\dagger\dagger}) \approx (p_0^{1/2}/\kappa \ln n)^{-3/4} \quad (71)$$

In turn, this roughly determines the core radius at the lower boundary of the regime of weak coronal confinement, $r_{\text{core}}(D_{\dagger\dagger})$. To this end, note that $r_{\text{core}} \approx (p\nu)^{1/3}$, $\nu \approx p_0^{1/2}a_0^{3/2}$, and $p = up_0$, thus leading to $r_{\text{core}} \approx u^{1/3}(p_0 a_0)^{1/2}$ and

$$r_{\text{core}}(D_{\dagger\dagger}) \approx (p_0^{1/2}/\kappa \ln n)^{-1/4} (p_0 a_0)^{1/2} < (p_0 a_0)^{1/2} \quad (72)$$

where $(p_0 a_0)^{1/2}$ is the unperturbed core radius in the $\kappa \ll 1$ limit.

Finally, for strong coronal confinement, $(n/p)^{3/5}b > D > r_{\text{core}}(u)$, the coronal penalty per amphiphile (Appendix I) is $F_{\text{corona}}/kT \approx n(b/D)^{5/3} + p \approx p_0^{2/3}(R_F/D)^{5/3}u^0 + p_0 u$. Narrowing the slit to $D < D_{\dagger\dagger}$ brings the system into this regime. In it

$$F_{\text{chain}}/kT \approx m\gamma a_0 [u^{1/3} + u^{-1/3} + \kappa u^{1/2} + (p_0\gamma a_0)^{-1}u^{-1} + t_{\text{sc}}u + (\gamma a_0)^{-1}n(b/D)^{5/3}] - m\delta \quad (73)$$

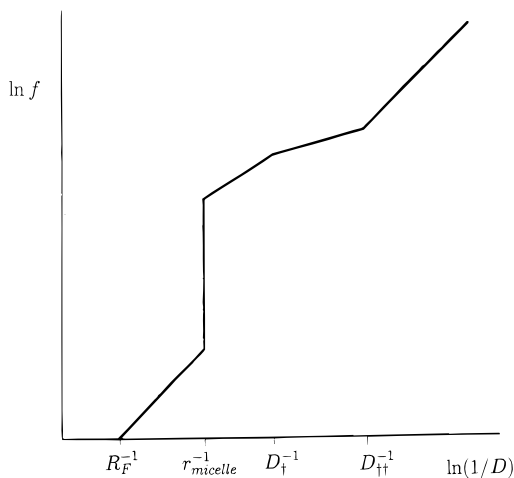


Figure 8. Variation of the restoring force per chain for a polysoap subject to confinement. $\ln f$ is plotted vs $\ln(1/D)$. For simplicity the initial Gaussian regime is not depicted.

where $t_{sc} \approx (p_0/\gamma a_0)$. t_{sc} is the ratio of the p dependent term in the strong confinement penalty of the micelles and $m\bar{\epsilon}_{p_0}$ at $p = p_0$ and a given D . The corresponding equilibrium condition is

$$u^{2/3} + \kappa u^{5/6} - (p_0/\gamma a_0)^{-1} u^{-2/3} + t_{sc} u^{4/3} \approx 1 \quad (74)$$

The coronal term is clearly dominant in this range, and for $D \ll D_{\dagger}$ we obtain $u \approx t_{sc}^{-3/4}$ or

$$u_{sc} \approx (\gamma a_0/p_0)^{3/4} \quad (75)$$

Note that $u_{sc} > 1/p_0$ so that the micelles are not fully dissociated. Since the logarithmic correction to the u term in F_{chain} was neglected, our analysis does not show a smooth crossover to the regime of weak coronal confinement. When we do allow for this correction, t_{sc} becomes $t_{sc} \approx (p_0/\gamma a_0) \{ \ln[(n/p_0 u)/D] - 3/5 \}$. In this form t_{sc} vanishes at D_{\dagger} , thus ensuring a smooth crossover. It also leads to a weak, logarithmic D dependence of u , which now decreases with D . However, when this negligible correction is ignored, we recover u_{sc} as given above. The lower boundary of this regime, $D_L \approx (p_0/\gamma a_0)^{1/4} a_0^{1/2}$ is set by the core radius, $r_{core} \approx u^{1/3} (p_0 a_0)^{1/2}$, for $u \approx u_{sc}$. In the strong coronal confinement range

$$F_{chain}/kT \approx m(\gamma a_0)^{3/4} p_0^{1/4} + p_0^{2/3} (R_F/D)^{5/3} \quad (76)$$

Knowing F_{chain} for the full range of slit widths, we may obtain the restoring force per chain $f = -\partial F_{chain}/\partial D$, in the various regimes (Figure 8).

$$\begin{aligned} f/kT &\approx R_F^2/D^3 \sim D^{-3} & R_F > D \gg r_{micelle} \\ f/kT &\approx R_F^{5/3}/D^{8/3} \sim D^{-8/3} & R_F \gg D > r_{micelle} \\ f/kT &\approx m p_0^{1/2} r_{micelle}^{5/8} / D^{13/8} \sim D^{-13/8} & r_{micelle} > D > D_{\dagger} \\ f/kT &\approx m(\ln n/\kappa)^{15/23} p_0^{1/2} r_{micelle}^{5/23} / D^{28/23} \sim D^{-28/23} & D_{\dagger} > D > D_{\ddagger} \\ f/kT &\approx p_0^{2/3} R_F^{5/3} / D^{8/3} \approx D^{-8/3} & D_{\ddagger} > D > D_L \end{aligned} \quad (77)$$

The first three regimes are indistinguishable from the behavior expected of a chain of stars. The micellar structure in this weak confinement range is only slightly

perturbed. The fourth regime exhibits a distinctive force law reflecting a strong coupling of the micellar structure and the micellar confinement. The final regime exhibits essentially the force law expected of the “bare” hydrophilic backbone. This is because the strong confinement of stars is, to lowest order, equivalent to the confinement of the “disconnected” arms. Accordingly, the strong confinement of the polysoap is dominated by the contribution of the “disconnected” spacer chains. In turn, this is clearly independent of the aggregation number. The aggregation number is weakly increasing in the first two regimes because the dominant penalty terms in this range are due to the confinement of the chain as a whole. These contributions are of the form $[R_F(u)/D]^y$ with $y > 1$. An increase of u makes for a smaller $R_F(u)$ and thus for a smaller elastic penalty. The subsequent three regimes are dominated by the micellar confinement. Of these, the first two are of the form $[r_{micelle}(u)/D]^y$ with $y < 1$. In these regimes, a decrease in u makes for smaller $r_{micelle}$ and thus for a smaller penalty. In the final regime, the strong confinement term exhibits a logarithmic dependence on the aggregation number, thus leading to a plateau in u .

VII. Discussion

The intramolecular self-assembly of polysoaps is expected to qualitatively modify their configurations and their elastic behavior. The effect on their elasticity reflects the existence of internal degrees of freedom. The response of the chain to perturbations involves the relaxation of the intrachain micelles in accordance with the LeChatelier principle. Qualitatively similar effects are expected in all flexible chains carrying numerous stickers, irrespective of the nature of the stickers. This general, thermodynamic argument does not allow us, however, to obtain the detailed force laws for the polysoaps. To this end, it is necessary to invoke a detailed statistical mechanics model. The model proposed in this article is clearly highly simplified: (i) The unperturbed chain is viewed as a linear string of spherical micelles. The analysis does not allow for other configurations. In particular, it does not allow for the most stable configuration corresponding to a spherical globule of close-packed micelles. (ii) The force law obtained assumes a thermodynamic equilibrium subject to geometrical constraints, *i.e.*, the deformation is assumed to be “quasi static”, that is, slow in comparison with the relaxation times of the intrachain micelles. Neither of these assumptions is likely to be fully satisfied in experimental situations. However, this approach is justified, at this early stage and in the absence of directly relevant experimental data, by its relative simplicity. In addition, we do expect some of the regimes considered to survive, irrespective of the precise configuration of the unperturbed chain. In particular, extension of globular or branched strings is expected to result, at an intermediate stage, in a linear string. Irrespective of the details, our considerations suggest that the deformation behavior of polysoaps should exhibit major deviations from that of the corresponding homopolymers. The direct experimental probe, by means of the surface force apparatus (SFA),²⁴ should be possible for the confinement behavior. In order to observe the single-chain behavior, it will be necessary to use sparsely grafted polysoaps. The extension behavior of isolated polysoaps is more difficult to study. The experimental methods that come to mind involve

the SFA in a shear mode²⁵ or the use of extensional flows.²⁶

Appendix I: Free and Confined Stars

Within the Daoud–Cotton model,¹⁸ an unperturbed star immersed in a good solvent is pictured as a sphere consisting of close-packed, impenetrable blobs. The blobs are arranged in concentric, spherical shells. Each of the p arms contributes a single blob to each shell. The size of a blob, ξ , in a shell of radius r is thus set by the requirement $r^2 \approx p\xi^2$, leading to

$$\xi(r) \approx r/p^{1/2} \quad (78)$$

Each blob contains $g \approx (\xi/b)^{5/3}$ monomers and thus $\xi \approx \phi^{-3/4}b$, where $\phi(r)$ is the local monomer volume fraction. As a result $\phi(r) \approx p^{2/3}(b/r)^{4/3}$. The radius, R , of a star having p arms consisting each of n monomers, is determined by the conservation of monomers, $N \approx \int_{r_{\text{core}}}^R g\xi^{-3}r^2 dr$ where $N = pn$ and r_{core} is the radius of the central, multifunctional site. This leads to

$$R \approx p^{1/5}n^{3/5}b \quad (79)$$

The total free energy of the corona of the star, F , as determined by the kT per blob ansatz is

$$F/kT \approx \int_{r_{\text{core}}}^R \xi^{-3}r^2 dr \approx p^{3/2} \ln(R/r_{\text{core}}) \approx p^{3/2} \ln n \quad (80)$$

The free energy per arm as used in the text applies to the limit of $R > r_{\text{core}}$ and is thus given by

$$F_{\text{corona}}/kT \approx p^{1/2} \ln(R/r_{\text{core}}) \approx p^{1/2} \ln n \quad (81)$$

A modified description applies to stars confined to a slit, of width D , formed by two nonadsorbing surfaces.^{27,28} The picture of a stratified array of blobs such that each arm contributes a single blob to each layer is retained. However, the confinement modifies the geometry of the layers and the structure of the blobs. Three coronal regions may be distinguished: (i) An inner region retaining the structure of the free star is found for $r < D$. In this region $\xi_f \approx r/p^{1/2}$ and $\xi_f \approx g^{3/5}b$. (ii) For $D < r < pD$ an intermediate region is found where the spherical symmetry is lost but the blobs retain their three-dimensional character, *i.e.*, $\xi_i \approx g^{3/5}b$. ξ_i is determined by equating the surface area of the cylindrical shell, rD , to $p\xi_i^2$, thus leading to

$$\xi_i \approx (rD/p)^{1/2} \quad (82)$$

At the upper boundary of this region, $r \approx pD$ and $\xi_i \approx D$, and for larger r values the confinement affects the structure of the blobs. (iii) An exterior, two-dimensional region extends beyond $r \approx pD$. It is characterized by cylindrical rather than spherical geometry. Furthermore, the blobs in this region are two-dimensional. Their in-plane span, $\xi_{||}$, is set by equating the circumference of a shell, r , to $p\xi_{||}$, thus leading to

$$\xi_{||} \approx r/p \quad (83)$$

Each two-dimensional $\xi_{||}$ blob consists of $(\xi_{||}/D)^{4/3} D$ blobs. In turn, each D blob incorporates $(D/b)^{5/3}$ monomers. Thus, the number of monomers in a $\xi_{||}$ blob is $g_{||} \approx (\xi_{||}/D)^{4/3}(D/b)^{5/3}$. The in-plane radius of the star is, again, determined by monomer conservation.

$$pn \approx \int_{r_{\text{core}}}^D g_{\text{f}} \xi_{\text{f}}^{-3} r^2 dr + \int_D^{pD} g_{\text{i}} \xi_{\text{i}}^{-3} rD dr + \int_{pD}^{R_{||}} g_{||} \xi_{||}^{-2} r dr \quad (84)$$

while the kT per blob ansatz determines the confinement free energy of the star

$$F_{\text{conf}}/kT \approx \int_{r_{\text{core}}}^D \xi_{\text{f}}^{-3} r^2 dr + \int_D^{pD} \xi_{\text{i}}^{-3} rD dr + \int_{pD}^{R_{||}} [1 + (\xi_{||}/D)^{4/3}] \xi_{||}^{-2} r dr \quad (85)$$

The asymptotic results obtained from the detailed analysis outlined above may also be derived by simpler arguments. These fail to obtain the local structure, $\xi(r)$ and $\phi(r)$, but afford greater convenience. To obtain $R_{||}$, we argue that it should obey the scaling form $R_{||} \approx R(R/D)^x$ where $R \approx p^{1/5}n^{3/5}b$. For $R/D \ll 1$, we further expect $R_{||} \sim n^{3/4}$ because of the onset of two-dimensional behavior. These requirements lead to $x = 1/4$ and thus

$$R_{||}/b \approx p^{1/4}n^{3/4}(b/D)^{1/4} \quad (86)$$

This form applies even when the two-dimensional region does not develop, for weak confinement such that $R_{||} < pD$, provided that the intermediate region is extended enough. In the strong confinement regime, the size of the exterior two-dimensional blobs is

$$\xi_{||} \approx R_{||}/p \approx p^{-3/4}n^{3/4}(b/D)^{1/4}b \quad (87)$$

The onset of this regime occurs when $\xi_{||} \approx D$ or

$$D_c \approx (n/p)^{3/5}b \quad (88)$$

It is possible to obtain the correct form for F_{conf} by ignoring the r dependence of $\xi_{||}$. Within this approximation the number of $\xi_{||}$ blobs is roughly $R_{||}^2/\xi_{||}^2 \approx p^2$. Actually, this estimate is accurate up to a logarithmic correction, as can be seen from the precise blob count $\int_{pD}^{R_{||}} \xi_{||}^{-2} r dr \approx p^2 \ln R_{||}/pD$. The number of $\xi_{||}$ blobs per arm is thus p , and each $\xi_{||}$ blob incorporates n/p monomers. Accordingly, the number of D blobs within a single $\xi_{||}$ blob is $(n/p)(b/D)^{5/3}$. Altogether, F_{conf} , as obtained by assigning kT to each D and $\xi_{||}$ blob, is roughly

$$F_{\text{conf}}/kT \approx p^2(n/p)(b/D)^{5/3} + p^2 \approx pn(b/D)^{5/3} + p^2 \quad (89)$$

The first term in this expression is dominant when $D < (n/p)^{3/5}b$. A more rigorous analysis, utilizing (85), reveals a logarithmic correction to the p^2 term in the form of a $\ln[(n/p)^{3/5}b/D]$ prefactor. This factor is due to the fact that $\xi_{||}$ is actually not a constant. It varies as $\xi_{||} \approx r$, thus giving rise to a self-similar structure. Accordingly, the p^2 term vanishes at the regime boundary $(n/p)^{3/5}b$. For strong confinements, $D \ll (n/p)^{3/5}b$, the logarithmic correction may be neglected, thus leading to (89). In the weak confinement regime, $R < D < (n/p)^{3/5}b$, the confinement free energy is expected to have the scaling form $F_{\text{conf}}/kT \approx p^{3/2}(R/D)^y$. At the crossover to the strong confinement regime, $D \approx D_c$, we expect $F_{\text{conf}}/kT \approx pn(b/D_c)^{5/3} \approx p^2$ and thus $y = 5/8$. Accordingly,

$$F_{\text{conf}}/kT \approx p^{3/2}(R/D)^{5/8} \approx p^{13/8}n^{3/8}(b/D)^{5/8} \quad (90)$$

This result may also be obtained by arguing that a confined star, occupying a volume of $R_{||}^2D$, consists of

close-packed, impenetrable blobs of size $\xi \approx \phi^{-3/4}b$, where $\phi \approx npb^3/DR_{\parallel}^2$.

Appendix II: Flory Radius of a Partially Dissociated String

To obtain R_F , we minimize the free energy per chain for a given ψ , F , with respect to R . F allows for two contributions. F_{el} reflects the Gaussian elasticity of a chain consisting of $m\psi/p$ micelles of size r_{micelle} and $mn(1 - \psi)$ monomers of size b

$$F_{el}/kT \approx R^2/[mn(1 - \psi)b^2 + (m\psi/p)r_{\text{micelle}}^2] \quad (91)$$

F_{int} accounts for the contribution of excluded volume interactions within the chain. Three types of interactions are involved: monomer–monomer, micelle–micelle, and monomer–micelle. The excluded volumes associated with the first two interactions are respectively b^3 and r_{micelle}^3 . Since $r_{\text{micelle}} \gg b$, the excluded volume for monomer–micelle interactions is well approximated by r_{micelle}^3 . Altogether

$$F_{\text{int}}/kT \approx R^{-3}[(\psi m/p)^2 r_{\text{micelle}}^3 + (\psi m/p)mn(1 - \psi)r_{\text{micelle}}^3 + m^2 n^2(1 - \psi)^2 b^3] \quad (92)$$

The equilibrium condition, $\partial F/\partial R = 0$, leads to

$$R^5 \approx (mn)^3[(1 - \psi)b^2 + (\psi/np)r_{\text{micelle}}^2] \times [(\psi/np)^2 r_{\text{micelle}}^3 + (\psi/np)(1 - \psi)r_{\text{micelle}}^3 + (1 - \psi)^2 b^3] \quad (93)$$

Since $r_{\text{micelle}} \approx p^{1/5}n^{3/5}b$

$$R_F/b \approx (mn)^{3/5}[(1 - \psi) + \psi n^{1/5}p^{-3/5}]^{1/5} \times [\psi^2 n^{-1/5}p^{-7/5} + \psi(1 - \psi)n^{4/5}p^{-2/5} + (1 - \psi)^2]^{1/5} \quad (94)$$

As $\psi \rightarrow 1$, this expression reduces to $R_F \approx (mn)^{3/5}p^{-2/5}b$ as $(mn)^{3/5}p^{-2/5}\psi^{3/5}b$. When $\psi \rightarrow 0$, R_F approaches $R_F \approx (mn)^{3/5}b$ as $R_F \approx (mn)^{3/5}(1 - \psi)^{3/5}$. One may approximate the full expression for R_F by retaining these two terms, i.e., $R_F \approx (mn)^{3/5}[p^{-2/5}\psi^{3/5} + (1 - \psi)^{3/5}]b$. This approximation underestimates R_F but retains the correct asymptotic behavior. However, this last expression is still too cumbersome to allow for an analytical solution for ψ . A convenient approximation is

$$R_F(\psi)/b \approx (mn)^{3/5}[p^{-2/3}\psi + (1 - \psi)]^{3/5} \approx (mn)^{3/5}p^{-2/5}[\psi(1 - p^{2/3}) + p^{2/3}]^{3/5} \approx R_F[\psi(1 - p^{2/3}) + p^{2/3}]^{3/5} \quad (95)$$

While this expression also underestimates R_F , it exhibits the correct asymptotic behavior and it yields a manageable expression for ψ .

Appendix III: A Little on the $\kappa \gg 1$ Case

To avoid unnecessary detail, we have confined the discussion in the main body of the article to the $\kappa \ll 1$ limit. The $\kappa \gg 1$ behavior may be obtained by straightforward modification of the $\kappa \ll 1$ results. In the following we present the main ingredients. Since this discussion concerns the conversion of results between the two limits, it is necessary to introduce an appropriate notation. We thus denote the equilibrium characteristics of the $\kappa \ll 1$ by a breve, while the corresponding quantities for the $\kappa \gg 1$ case are marked by a circumflex

(hat). For example, the Flory radius in the two limits will be denoted respectively by \hat{R}_F and by \breve{R}_F .

In the $\kappa \gg 1$ limit, the coronal penalty in ϵ_p , as given by (7), is dominant. Consequently, this term, $\kappa u^{1/2}$, is comparable to the surface term, $u^{-1/3}$. Accordingly, $\hat{u} \approx \kappa^{-6/5}$ and the corresponding micellar characteristics are

$$\hat{p} \approx p_0 \kappa^{-6/5} \quad (96)$$

$$\hat{a} \approx a_0 \kappa^{2/5} \quad (97)$$

$$\hat{r}_{\text{core}} \approx \hat{p}^{1/2} \hat{a}^{1/2} \approx \breve{r}_{\text{core}} \kappa^{-2/5} \quad (98)$$

$$\hat{r}_{\text{micelle}} \approx \hat{p}^{1/5} n^{3/5} b \approx \breve{r}_{\text{micelle}} \kappa^{-6/25} \quad (99)$$

The two relevant chain dimensions are

$$\hat{R}_F \approx (m/\hat{p})^{3/5} \hat{r}_{\text{micelle}} \approx \breve{R}_F \kappa^{12/25} \quad (100)$$

$$\hat{R}_{\text{max}} \approx (m/\hat{p}) \hat{r}_{\text{micelle}} \approx R_{\text{max}} \kappa^{24/25} \quad (101)$$

The general expressions for F_{chain} , as given by (14), (59), (63), and (73), are valid for any κ . Accordingly, it is not surprising that the general features of the fR and fD diagrams remain the same. This applies to the sequence of regimes and to the R or D dependence of f in each of them. The distinctive features of the $\kappa \gg 1$ limit concern the position of the domain boundaries and the value of numerical prefactors such as the “spring constants”. These may be obtained, by following dimensional considerations, by replacing p_0 by \hat{p} , a_0 by \hat{a} , \breve{R}_F by \hat{R}_F , etc. in the relevant expressions. For example, \hat{R}^* is specified by

$$\hat{\tau}(\hat{R}^*) \approx 1 \quad (102)$$

where $\hat{\tau}$ is the ratio of the elastic free energy, \hat{F}_{el} , and the micellar free energy, $m\epsilon_{\hat{p}}$ for a weakly perturbed chain with $\hat{u} \approx \kappa^{-6/5}$ etc. This leads to

$$\hat{R}^* \approx \hat{p}^{1/5}(\gamma \hat{a})^{2/5} \hat{R}_{\text{max}} > \hat{R}_{\text{max}} \quad (103)$$

Acknowledgment. O.V.B. acknowledges with thanks the hospitality of Prof. K. Kremer and the Max Planck Institut für Polymerforschung.

List of Symbols

a = area per one amphiphile at the micellar core–water interface
 a_0 = optimal surface area in the micelle formed by nonpolymerized amphiphiles
 b = monomer length
 D = width of the slit
 D_{\uparrow} = slit width defined from the condition $t_{wc}(D_{\uparrow}) \cong 1$
 $D_{\uparrow\uparrow}$ = slit width defined from the condition $D_{\uparrow\uparrow} \cong (n/p)^{3/5}b$
 f = tension in the chain
 f_{co} = tension at coexistence with disregarding of mixing entropy
 \tilde{f}_{co} = tension at coexistence if the mixing entropy is taken into account
 F_{chain} = free energy of the polysoap chain
 $F_0 = kTm\epsilon_{p_0}$ = micellar contribution in the completely aggregated state
 $F_{\text{micelle}} = kTm\psi\epsilon_{p_0}$ = micellar contribution in the partially dissociated state
 F_{el} = elastic (conformational) contribution to the free energy of the extended polysoap
 F_{corona} = free energy of steric repulsion in the micellar corona per one amphiphilic monomer

F_{conf} = confinement free energy of the polysoap molecule
 k = Boltzmann constant
 m = number of amphiphilic monomers in the polysoap chain
 m_u = number of amphiphilic monomers in the chain supporting, on average, a single dissociated micelle at zero tension
 n = number of monomers in a spacer
 n_d = number of dissociated micelles
 p = number of amphiphilic monomers per micelle
 p_0 = the optimal aggregation number of amphiphilic monomers in the micelle formed by nonpolymerized amphiphiles
 r_{core} = radius of the micellar core
 $r_{\text{micelle}} \cong n^{3/5} p^{1/5} b$ = radius of the micellar corona
 R = end-to-end distance (extension) of the polysoap molecule
 $R_F(p) \cong (m/p)^{3/5} r_{\text{micelle}}$ = Flory radius of the polysoap molecule consisting of intramolecular micelles with aggregation number p
 R_F = Flory radius for the polysoap molecule consisting of intramolecular micelles of aggregation number p_0
 $R_F(\psi) = R_F[\psi(1 - p_0^{2/3}) + p_0^{2/3}]^{3/5}$ = Flory radius of the partially dissociated chain
 $R_B(u) \cong (mn/p)^{3/5}$
 $R_B \cong (mn/p_0)^{3/5}$
 $R_B(\psi) \cong R_B[p_0 + (1 - p_0)\psi]^{3/5}$
 $R_{\text{max}}(p) \cong (m/p) r_{\text{micelle}}$ = maximal extension of the chain of micelles of aggregation number p
 $R_{\text{max}} = R_{\text{max}}(p)$ for $p = p_0$
 R_L = lower boundary of the coexistence region under the condition of disregarding of mixing entropy
 R_U = upper boundary of the coexistence region under the condition of disregarding of mixing entropy
 \tilde{R}_L = lower boundary of the coexistence region with mixing entropy taken into account
 \tilde{R}_U = upper boundary of the coexistence region with mixing entropy taken into account
 \tilde{R} = extension of the chain at coexistence when mixing entropy is taken into account
 R^* = defined from the condition $\tau(R^*) \cong 1$
 R^{**} = defined from condition $p = 1$ under the assumption of a uniform decrease of the aggregation number under extension
 S_{mix} = entropy of mixing of micelles and dissociated amphiphiles in the chain at coexistence
 $S_{\text{mix}} = dS_{\text{mix}}/d\psi$
 $t_{\text{wc}} \cong (\gamma a_0)^{-1} p_0^{1/2} (r_{\text{micelle}}/D)^{5/8}$ = perturbation parameter at weak confinement
 $t_{\text{sc}} \cong (p_0/\gamma a_0)$
 T = temperature
 $u = p/p_0$ = reduced aggregation number
 v = volume of the hydrophobic tail of the amphiphilic monomer
 γ = surface tension in kT units
 $-\delta$ = transfer free energy for the hydrophobic tail from water to the micellar core
 $\tilde{\epsilon}_p$ = free energy per surfactant in a micelle of aggregation number p
 ϵ_p = free energy per amphiphilic monomer in an intrachain micelle of aggregation number p

ψ = fraction of aggregated amphiphilic monomers at coexistence
 $\bar{\psi}$ = fraction of aggregated monomers at zero tension

$\tau(R) \cong F_{\text{el}}(R)/m\gamma a_0$ = perturbation parameter for extension

References and Notes

- (1) Flory, P. *Principles of Polymer Chemistry*; Cornell University Press: Ithaca, NY, 1953.
- (2) de Gennes, P. G. *Scaling Concepts in Polymer Physics*; Cornell University Press: Ithaca, 1979.
- (3) Napper, D. H. *Polymeric Stabilization of Colloidal Suspensions*; Academic Press: New York, 1983.
- (4) Doi, M.; Edwards, S. F. *The Theory of Polymer Dynamics*; Clarendon: Oxford, U.K., 1986.
- (5) Kuhn, W. *Kolloid Z.* **1936**, 76, 258; **1939**, 87, 3.
- (6) Kuhn, W.; Gr \ddot{u} n, F. *Kolloid Z.* **1942**, 101, 248.
- (7) Guth, E.; Mark, H. *Monatsh. Chem.* **1934**, 65, 93.
- (8) James, H. M.; Guth, E. *J. Chem. Phys.* **1943**, 11, 470.
- (9) Borisov, O. V.; Halperin, A. *Europhys. Lett* **1996**, 34, 657.
- (10) Borisov, O. V.; Halperin, A. *Macromol. Symp.*, in press.
- (11) (a) Bader, H.; Dorn, K.; Hupfer, B.; Ringsdorf, H. *Adv. Polym. Sci.* **1985**, 64, 1. (b) Gros, L.; Ringsdorf, H.; Scupp, H. *Angew. Chem., Int. Ed. Engl.* **1981**, 20, 305. (c) Laschewsky, A. *Adv. Polym. Sci.* **1995**, 124, 1. (d) Hogen-Esch, T. E.; Amis, E. *Trends Polym. Sci.* **1995**, 3, 98. (e) Glass, J. E., Ed. *Polymers in Aqueous Media: Performance Through Association*; American Chemical Society: Washington, DC, 1989. (f) Goddard, E. D.; Ananthapadmanabhan, K. P., Eds. *Interactions of Surfactants with Polymers and Proteins*; CRC Press: Boca Raton, FL, 1993. (g) Glass, J. E., Ed. *Hydrophilic Polymers: Performance with Environmental Acceptance*; American Chemical Society: Washington, DC, 1996.
- (12) Borisov, O. V.; Halperin, A. *Langmuir* **1995**, 11, 2911.
- (13) Borisov, O. V.; Halperin, A. *Macromolecules* **1996**, 29, 2612.
- (14) Landau, L. D.; Lifshitz, E. M. *Statistical Physics*; Pergamon Press: Oxford, U.K., 1986.
- (15) Reif, F. *Fundamentals of Statistical and Thermal Physics*; McGraw-Hill: London, 1965.
- (16) Borisov, O. V.; Halperin, A. *Macromol. Symp.*, in press.
- (17) Israelachvili, J. N. *Intramolecular and Surface Forces*, 2nd ed.; Academic Press: London, 1991.
- (18) (a) Daoud, M.; Cotton, J. P. *J. Phys. Fr.* **1982**, 43, 531. (b) Zhulina, E. B. *Polym. Sci. USSR* **1984**, 26, 794. (c) Birshtein, T. M.; Zhulina, E. B. *Polymer* **1984**, 25, 1453.
- (19) Halperin, A. *Macromolecules* **1987**, 20, 2943.
- (20) Strictly speaking, ϵ_p should also reflect a contribution due to the overall configuration of the chain. However, for a linear string of micelles, this contribution is negligible, as was discussed in ref 12.
- (21) For an estimate of κ , see ref 12. Note that κ depends on the choice of amphiphiles, via p_0 , and on the length of the spacer chains, n . A rough estimate suggests that $\kappa \approx 1$ for SDS and $n \approx 10$.
- (22) Pincus, P. *Macromolecules* **1976**, 9, 386.
- (23) Daoud, M.; de Gennes, P. G. *J. Phys. (Les Ulis, Fr.)* **1976**, 35, 85.
- (24) Patel, S. S.; Tirrell, M. *Annu. Rev. Phys. Chem.* **1989**, 40, 597.
- (25) Klein, J. *Annu. Rev. Mater. Sci.* **1996**, 26, 581.
- (26) Nguyen, T. Q.; Kaush, H. H., Eds. *Flexible Polymers in Elongational Flow: Theories and Experiments*; Springer Verlag: Heidelberg, 1996.
- (27) Halperin, A.; Alexander, S. *Macromolecules* **1987**, 20, 1146.
- (28) Halperin, A.; Joanny, J. F. *J. Phys. Fr. II* **1991**, 1, 623.

MA961670L